International Journal of Biomedicine 16(3) (2026) 372-377
http://dx.doi.org/10.21103/Article16(3)_OA7

ORIGINAL ARTICLE

INTERNATIONAL JOURNAL OF BIOMEDICINE

Ginsenoside Rg3 Induces Apoptosis While Attenuates Collagen Metabolism in Human Vocal Cord Scar Fibroblasts In Vitro

Yan Qin[1], Kang Wang[1], Zhi-Mao Zhang [1], Ting Wu[2], Long Zhang[1], Jun Liu[1*]

[1]*Department of Otorhinolaryngology Head and Neck Surgery, Yichang Central People's Hospital ,The First College of Clinical Medical Science, China Three Gorges University, 443000, Yichang, China*

[2]*Department of Otorhinolaryngology Head and Neck Surgery, Nanjing Tongren Hospital, School of Medicine, Southeast University, 211102, Nanjing, China*

Abstract

Background: This study aimed to investigate the effects of ginsenoside Rg3 on apoptosis and collagen metabolism in human vocal cord scar fibroblasts (HVCSFs) and the molecular mechanisms involved.
Methods and Results: HVCSFs were cultured in vitro and treated with different concentrations of ginsenoside Rg3. Cell proliferation inhibition rate was detected by CCK-8 assay. Cell apoptosis was analyzed by flow cytometry and Calcein/PI live/dead cell staining. Cell invasion ability was detected by Transwell assay. Expression levels of apoptosis-related protein caspase-3 and Collagen Type I, Collagen Type III (Col I, Col III) were detected by Western blot and Quantitative real-time polymerase chain reaction (qPCR). HVCSFs were cultured in vitro and exposed to increasing concentrations of ginsenoside Rg3. Rg3 treatment dose-dependently inhibited HVCSFs proliferation, as shown by the CCK-8 assay ($P<0.0001$). Flow cytometry and Calcein/PI live/dead staining consistently revealed a significant induction of apoptosis upon Rg3 exposure ($P<0.0001$). Cell invasion was also effectively suppressed, as assessed by the Transwell assay ($P<0.001$, $P<0.0001$). At the protein level, Western blot analysis demonstrated that Rg3 upregulated caspase 3 expression ($P<0.01$, $P<0.001$) while downregulating both Col I and Col III ($P<0.05$, $P<0.01$). Correspondingly, qPCR results showed elevated mRNA levels of caspase 3 ($P<0.05$, $P<0.01$, $P<0.0001$) and reduced mRNA levels of Col I and Col III ($P<0.05$, $P<0.0001$) in response to Rg3 treatment.
Conclusions. Ginsenoside Rg3 may promote the apoptosis of HVCSFs through activating the caspase-3-dependent apoptotic pathway and inhibiting the expression of Col I and Col III, thereby improving vocal cord scar fibrosis. This study provides experimental evidence for ginsenoside Rg3 as a potential anti-vocal cord scar drug.(**International Journal of Biomedicine. 2026;16(3):372-377.**)

Keywords: ginsenoside Rg3 • vocal cord scar • fibroblasts • apoptosis • collagen metabolism

For citation: Qin Y, Wang K, Zhang Z-M, Wu T, Zhang L, Liu J. Ginsenoside Rg3 Induces Apoptosis While Attenuates Collagen Metabolism in Human Vocal Cord Scar Fibroblasts In Vitro. International Journal of Biomedicine. 2026;16(3):372-377. doi:10.21103/Article16(3)_OA7

Introduction

Vocal fold scarring refers to the pathological fibrosis of the extracellular matrix within the lamina propria, leading to impaired vibratory function and voice disorders.[1,2] It is commonly caused by surgical trauma (e.g., vocal fold resection),[3] prolonged intubation, chronic inflammation, or radiation therapy. Scar tissue disrupts the viscoelastic properties of the vocal folds, resulting in symptoms such as hoarseness, vocal fatigue, reduced vocal range, and breathiness. Although various clinical interventions have been tested for the treatment of voice disorders and vocal fold paralysis,[4-8] satisfactory restoration of vocal fold function remains elusive. Current therapeutic options are limited, necessitating the development of novel approaches to promote vocal fold healing and functional recovery.

Ginsenoside Rg3, a bioactive compound enriched from steamed or heated Panax ginseng roots, exhibits multiple pharmacological effects, including anti-angiogenic, anti-tumor, and anti-fibrotic properties.[9-11] Previous studies have demonstrated that ginsenoside Rg3 inhibits fibroblast proliferation and migration while inducing apoptosis, thereby modulating the expression of proteins and mRNA levels associated with proliferation, apoptosis, and migration.[12,13]

Additionally, ginsenoside Rg3 has been shown to suppress fibroblast proliferation, angiogenesis, and collagen synthesis via the TGF-β1/Smad and ERK signaling pathways.[14] Histologically, the composition and distribution of the extracellular matrix (ECM) in the lamina propria are essential for maintaining the viscoelastic properties required for vocal fold vibration. The ECM comprises hyaluronic acid (HA), collagen, elastin, fibronectin, and other components.[7,15] Specifically, HA maintains viscoelasticity and functions as a shock absorber, collagen provides structural support, and elastin preserves vocal fold vibration through its intrinsic elasticity.

This study aims to verify whether ginsenoside Rg3 can reduce human vocal fold scarring and explore the underlying mechanisms by which ginsenoside Rg3 regulates scar formation in human vocal folds.

Materials and Methods

Chemicals

Ginsenoside Rg3 (purity ≥99.5%) was obtained from Wuhan Jingbiao Technology Co., Ltd. (Wuhan, China). Rg3 powder was dissolved in dimethyl sulfoxide (DMSO) to prepare a stock solution, which was then sterilized by filtration through a 0.22 μm polyethersulfone (PES) membrane filter. The stock solution was serially diluted with complete cell culture medium to achieve final Rg3 concentrations of 10, 20, 40, 80, and 160 μg/mL. The final concentration of DMSO in all treatment groups was maintained at 0.05% (v/v). A vehicle control group containing 0.05% DMSO without Rg3 was used as the negative control.

Cell culture

Human vocal cord scar fibroblasts (HVCSFs) were obtained from iCell Bioscience Inc. (Shanghai, China). Cells were maintained in high-glucose Dulbecco's Modified Eagle Medium (DMEM; HyClone, China) supplemented with 10% fetal bovine serum (FBS; Solarbio, China) and cultured at 37°C in a humidified atmosphere containing 5% CO_2. The medium was refreshed every 2–3 days, and cells were passaged when reaching 80–90% confluence.

Cell viability assay

Cell viability was evaluated using the Cell Counting Kit-8 assays (CCK-8; Bioswamp Life Science, China) according to the manufacturer's instructions. Briefly, HVCSFs were seeded in 96-well plates at a density of 3×10^3 cells per well in 100 μL of complete medium and incubated at 37°C in a humidified atmosphere with 5% CO_2 for 24 h to allow complete attachment. The medium was then replaced with fresh medium containing Rg3 at final concentrations of 0 (vehicle control), 10, 20, 40, 80, and 160 μg/mL. At designated time points (24, 48, and 72 h post-treatment), 10 μL of CCK-8 reagent was added to each well, and plates were incubated for an additional 1–4 h at 37°C. The absorbance at 450 nm was measured using a microplate reader (Allsheng, China). Cell viability was calculated using the following formula: Cell viability (%) = [(OD_control - OD_treated) / (OD_control - OD_blank)] × 100%. Each treatment group was assayed in quintuplicate, and experiments were repeated independently at least three times.

Flow Cytometry

Cell cycle analysis: HVCSFs (1×10^7 per group) were harvested, washed with PBS, and fixed in 75% ethanol at -20°C for at least 24 h. After washing twice with PBS, cells were stained with 0.5 mL PI/RNase Staining Buffer (BD Biosciences, USA) for 15 min at room temperature in the dark. DNA content was analyzed using a flow cytometer (ACEA NovoCyte, China), and cell cycle distributions were determined using NovoExpress software (ACEA Biosciences, China).

Apoptosis detection: Cell apoptosis was assessed using an Annexin V-FITC/PI Apoptosis Detection Kit (BD Biosciences, USA). After 48 h of treatment, HVCSFs were collected and resuspended in 1× Annexin V Binding Buffer. Annexin V-FITC (5 μL) and PI (5 μL) were added according to the manufacturer's instructions. After incubation for 15 min at room temperature in the dark, cells were analyzed by flow cytometry (ACEA NovoCyte, China). Data were analyzed using NovoExpress software (Allsheng, China).

Calcein-AM/Propidium Iodide (PI) staining

Cell viability was evaluated using the Calcein-AM/PI Double Staining Kit (C2015S, Beyotime Biotechnology, China) according to the manufacturer's instructions. Briefly, treated HVCSFs were washed twice with PBS and incubated with a working solution containing Calcein-AM (2 μM) and PI (4.5 μM) at 37°C for 30 min in the dark. After incubation, cells were washed once with PBS to remove excess dye and immediately visualized under an inverted fluorescence microscope (Nikon Ts2/Ts2-FL, Japan) equipped with appropriate filter sets. Calcein-AM-positive live cells (green fluorescence, excitation/emission = 494/517 nm) and PI-positive dead cells (red fluorescence, excitation/emission = 535/617 nm) were captured using NIS-Elements software (Nikon, Japan). Representative images from at least three independent experiments were recorded.

Transwell assay

Cell invasion assay: HVCSFs (2×10^4 cells in 200 μL serum-free DMEM) were seeded into the upper chamber of a Matrigel-coated Transwell insert (8 μm pore size; BD Biosciences, USA). The lower chamber contained 600 μL DMEM with 10% FBS as a chemoattractant. After 24h incubation at 37°C, invaded cells were fixed with 4% paraformaldehyde and stained with 0.1% crystal violet. Invaded cells were quantified by counting five random fields per insert under an inverted microscope (Nikon, Japan).

Cell migration assay: Transwell chambers (8 μm pore size; Corning, USA) were pre-hydrated with PBS for 5 min. HVCSFs (1×10^5 cells in 0.5 mL medium with 1% FBS) were seeded into the upper chamber, while the lower chamber contained 0.75 mL complete medium with 10% FBS. After 24 h incubation at 37°C, non-migrated cells were removed from the upper surface. Migrated cells were fixed with 4% paraformaldehyde (20 min, RT), stained with 0.5% crystal violet (30 min), and counted under 200× magnification (five random fields per chamber).

Quantitative real-time PCR (qPCR)

Total RNA of HVCSFs was extracted using TRIzol Reagent (Ambion, USA) and quantified with a Nano-300 micro-spectrophotometer (Aosheng, China). Genomic DNA

was removed using 5× gDNA digester Mix (YEASEN, China) at 42°C for 2 min. First-strand cDNA was synthesized using Hifair® III 1st Strand cDNA Synthesis SuperMix (YEASEN, China) in a 20 μL reaction containing 15 μL digested RNA and 5 μL 4× SuperMix at 25°C for 5 min, 55°C for 15 min, and 85°C for 5 min. qCR was performed on a CFX-Connect 96 system (Bio-Rad, USA) using Hieff® qPCR SYBR® Green Master Mix (No Rox) (YEASEN, China). Each 20 μL reaction contained 10 μL Master Mix, 0.5 μL each primer (10 μM), 1 μL cDNA, and 8 μL DNase/RNase-free water. The cycling conditions were: 95°C for 3 min, followed by 40 cycles of 95°C for 5 s, 56°C for 10 s, and 72°C for 25 s. Melting curve analysis was performed to verify specificity. GAPDH served as the internal reference, and relative expression of Collagen Type(Col)I, Col III, and Caspase-3 was calculated using the $2^{-\triangle\triangle ct}$ method. qPCR primer sequences are listed in Table 1.

Table 1.

The information on the primers used of qPCR

Gene	Sequence	Size of amplified fragment (bp)
Col I-F	5'-GAGATGGTGTTGATGGTCCC-3'	100
Col I-R	3'-GCAGCAAAGTTCCCAGTAAGA-5'	
Col III-F	5'-TGCCCACAGCCTTCTACAC-3'	111
Col III-R	3'-GCCAGGGTCACCATTTCT-5'	
Caspase-3-F	5'-GGTTCATCCAGTCGCTTT-3'	99
Caspase-3-R	3'-ATTCTGTTGCCACCTTTC-5'	
GAPDH-F	5'-GGGAAACTGTGGCGTGAT-3'	299
GAPDH-R	3'-GAGTGGGTGTCGCTGTTGA-5'	

Western Blotting

Protein samples were extracted from HVCSFs using RIPA lysis buffer (Bioswamp, China) supplemented with protease and phosphatase inhibitors (Bioswamp, China), followed by centrifugation at 12,000×g for 15 min at 4°C. Protein concentrations were determined using the BCA protein assay kit (Bioswamp, China) according to the manufacturer's instructions, with absorbance measured at 562 nm. Equal amounts of protein (20 μg per lane) were mixed with 5× loading buffer (Bioswamp, China), denatured by boiling for 10 min, and separated on 10% SDS-PAGE gels prepared using a one-step PAGE gel preparation kit (Bioswamp, China). Electrophoresis was performed at a constant voltage of 300 V for 20 min using rapid electrophoresis buffer (Bioswamp, China). Proteins were then transferred to PVDF membranes (Bioswamp, China) using rapid transfer buffer (Bioswamp, China) at 400 mA for 15–30 min in a wet transfer system. After blocking with protein-free rapid blocking solution (Bioswamp, China) for 10 min at room temperature, membranes were incubated with primary antibodies against Col I, Col III, Caspase-3, or GAPDH (1:1000, Bioswamp, China) diluted in primary antibody dilution buffer (Bioswamp, China) for 1 h at room temperature. Following three washes with PBST (5 min each), membranes were incubated with HRP-conjugated secondary antibodies (goat anti-rabbit IgG, 1:20000, Biosharp, China; goat anti-mouse IgG, 1:20000, Bioswamp, China) for 1 h at room temperature, washed three times with PBST (5 min each), and visualized using Super ECL Plus chemiluminescence detection kit (Bioswamp, China). Immunoreactive bands were captured using a fully automated chemiluminescence analyzer (Tanon-5200, China), and band intensities were quantified with ImageJ software.

Statistical analysis

All experiments were independently conducted in triplicate to ensure reproducibility. Each data represents the mean value derived from three independent replicates, and results are presented as mean ± standard deviation (SD). Differences among multiple groups were analyzed using one-way analysis of variance (ANOVA) followed by post-hoc Tukey's honestly significant difference (HSD) test for multiple comparisons. Differences with a *P*-value of <0.05 were considered statistically significant (*$P < 0.05$, ** $P < 0.01$, *** $P < 0.001$,****$P < 0.0001$). All analyses were performed using GraphPad Prism 10.4.2 (GraphPad Software, USA).

Results

Ginsenoside Rg3 exhibits concentration-dependent inhibition of the proliferation of HVCSFs and promotion of their apoptosis.

We treated HVCSFs with 0, 10, 20, 40, 80, and 160 μg/mL Ginsenoside Rg3, detected the cell proliferation inhibition rate using the CCK-8 method, analyzed the apoptosis situation by flow cytometry and Calcein/PI live/dead cell staining, tested the invasion ability of cells by Transwell assay, and detected the expression level of apoptosis-related protein caspase-3 by Western blot and qPCR. CCK-8 showed that after 24 hours, with the increase in drug concentration, the inhibition rate further rose from approximately 19.98% to 44.55% (Figure 1A) (P <0.0001), while following a 48-hour exposure to the drug, the inhibition rate elevated from 40.32% to 61.80% (Figure 1A)(P <0.0001). Flow cytometry and Calcein/PI indicated that with the increase of Ginsenoside Rg3 concentration, the apoptosis of HVCSFs increased (Figure 1B-C) (P < 0.0001). Transwell assay showed that with the increase of Ginsenoside Rg3 concentration, the number of invaded cells gradually decreased (figure 2A) ($P_{10\ \mu g/mL}$=0.0896, $P_{20\ \mu g/mL}$<0.0001, $P_{40\ \mu g/mL}$<0.0001, $P_{80\ \mu g/mL}$=<0.0001, $P_{160\ \mu g/mL}$<0.0001) the number of migrated cells also revealed a similar trend(figure 2B) ($P_{10\ \mu g/mL}$=0.0518, $P_{20\ \mu g/mL}$<0.0001, $P_{40\ \mu g/mL}$<0.0001, $P_{80\ \mu g/mL}$=<0.0001, $P_{160\ \mu g/mL}$<0.0001)qPCR indicated that Ginsenoside Rg3 upregulated the expression of caspase-3 in a concentration-dependent manner(figure 3A)($P_{10\ \mu g/mL}$=0.0089, $P_{20\ \mu g/mL}$=0.0064, $P_{40\ \mu g/mL}$=0.0047, $P_{80\ \mu g/mL}$=0.0021, $P_{160\ \mu g/mL}$=0.0005), Western blot results showed that Ginsenoside Rg3 also enhanced the expression of caspase-3 protein(figure 3B-C) ($P_{10\ \mu g/mL}$=0.8259, $P_{20\ \mu g/mL}$=0.0234, $P_{40\ \mu g/mL}$=0.0096, $P_{80\ \mu g/mL}$<0.0001, $P_{160\ \mu g/mL}$<0.0001).

Ginsenoside Rg3 inhibits the excessive deposition of extracellular matrix in HVCSFs.

In normal vocal cords, Col I is the main type of collagen, providing high strength and tensile resistance, maintaining the

mechanical stability of the vocal cords, and enabling them to withstand vibrations and tension during speech. Col III usually coexists with Col I to form a finer fiber network, increasing the elasticity and flexibility of the tissue, and facilitating the adaptability of vocal cord vibrations. The mRNA transcription levels of the genes encoding these two types of collagens (Col I and Col III) were typically detected using qPCR. The results showed that after Rg3 treatment, Col I mRNA levels in HVCSFs were significantly downregulated. This inhibitory effect was also dose-dependent (Figure 3 A) ($P_{10\ \mu g/mL}$=0.0082, $P_{20\ \mu g/mL}$=0.0104, $P_{40\ \mu g/mL}$=0.0064, $P_{80\ \mu g/mL}$=0.0037, $P_{160\ \mu g/mL}$=0.0015) and the mRNA level trend of Col III was similar to that (figure 3 A) ($P_{10\ \mu g/mL}$=0.0062, $P_{20\ \mu g/mL}$=0.0033, $P_{40\ \mu g/mL}$=0.0021, $P_{80\ \mu g/mL}$=0.0304, $P_{160\ \mu g/mL}$=0.0011). We performed the Western blot experiment, and the results showed that a higher concentration of Rg3 significantly inhibited the Col I protein level in HVCSFs (Figure 3 B-C) ($P_{10\ \mu g/mL}$=0.1217, $P_{20\ \mu g/mL}$=0.0466, $P_{40\ \mu g/mL}$=0.0188, $P_{80\ \mu g/mL}$<0.0001, $P_{160\ \mu g/mL}$<0.0001), while the Col III protein level exhibited a similar trend (figure 3 B-C) ($P_{10\ \mu g/mL}$=0.0998, $P_{20\ \mu g/mL}$=0.0606, $P_{40\ \mu g/mL}$=0.0339, $P_{80\ \mu g/mL}$<0.0001, $P_{160\ \mu g/mL}$<0.0001).

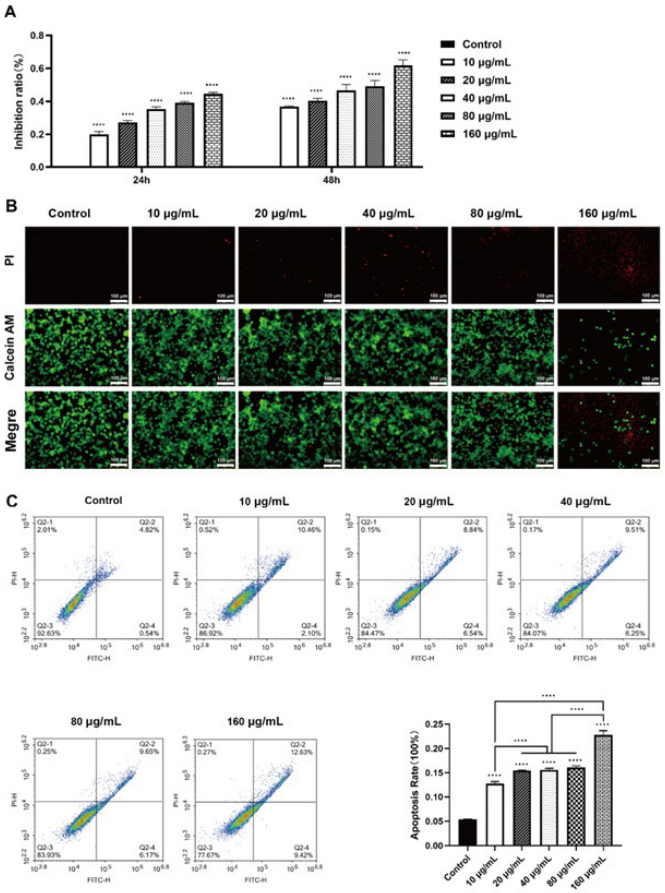

Figure1. *Rg3 inhibited the proliferation of Human vocal cord scar fibroblasts (HVCSFs) and promoted their apoptosis. A: The inhibition ratio of constructed with the Cell Counting Kit-8 assays(CCK-8) results after Rg3 treatment for 24 h and 48h, B: Fluorescence images of HVCSFs dual-stained with calcein AM (green) and PI (red) at 48 h after Rg3 treatment (10×, Scale bar =100* **μm**), *C: Flow cytometry analysis of apoptosis and the corresponding apoptosis rates in HVCSFs were obtained after 48 h after Rg3 treatment (****P < 0.0001).*

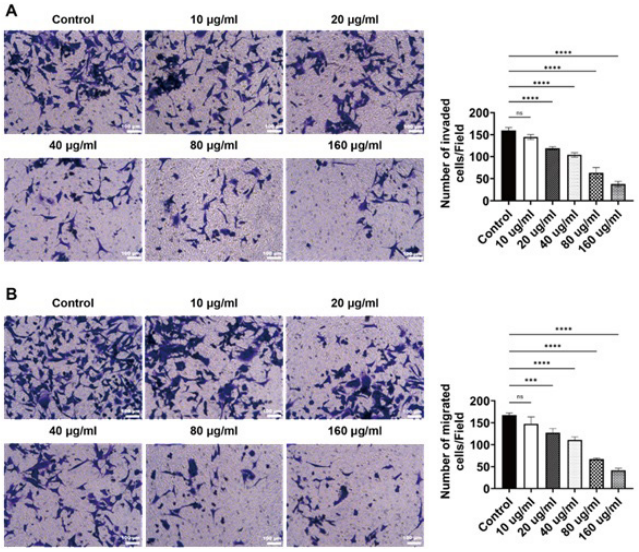

Figure 2. *The migration and invasion abilities of HVCSFs were assayed in Transwell chambers after Rg3 treatment, A: the Transwell invaded, B: the Transwell migrated (200×, Scale bar =100* μm, *** *P < 0.001,**** P< 0.0001).*

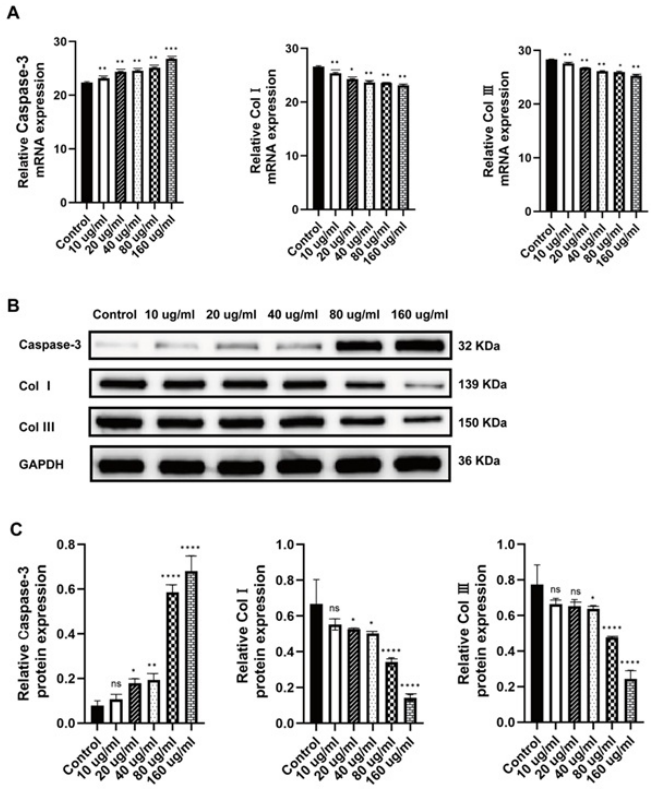

Figure 3. *Effects of Rg3 on Collagen Type (Col) I, Col III, and Caspase-3 signaling activities in cultured HVCSFs. A: It showed mRNA relative expression levels of Col I, Col III, and Caspase-3 in HVCSFs at treated with different concentrations of Rg3 (10, 20, 40, 80, and 160 μg/mL). B: Protein levels of Col I, Col III, and Caspase-3 in HVCSFs at treated with different concentrations of Rg3. C: Densitometric analysis of (B). (*P< 0.05, ** P < 0.01, *** P < 0.001,**** P < 0.0001).*

Discussion

The present study demonstrated that ginsenoside Rg3 exerts significant inhibitory effects on the proliferation of human vocal fold scar fibroblasts (HVFSFs), while promoting their apoptosis in a concentration-dependent manner. Additionally, Rg3 effectively suppressed the excessive deposition of Col I and Col III, key ECM components that contribute to vocal fold fibrosis. These findings suggest that Rg3 may serve as a potential therapeutic agent for vocal fold scarring by modulating fibroblast activity and collagen metabolism.

The results of this study indicate that ginsenoside Rg3 has a dual regulatory effect on HVCSFs, providing important clues for a deeper understanding of its therapeutic mechanism. Firstly, Rg3 dose-dependently inhibited the proliferation of HVCSFs and significantly promoted cell apoptosis. The Caspase (Cysteine-dependent aspartate-directed proteases) family is a core molecule in the apoptotic signaling pathway. Among them, Caspase-3 is regarded as the key executor of apoptosis, and its activation marks an irreversible "dead end" in the process of cell apoptosis.[16] Western blot and qPCR analyses confirmed that the expression of the apoptotic execution molecule caspase-3 was significantly upregulated after Rg3 treatment, suggesting that Rg3 may actively induce the programmed death of over-proliferating vocal cord scar fibroblasts by activating the caspase-3-dependent apoptotic pathway. Furthermore, the regulatory effect of Rg3 on collagen metabolism is particularly significant. The study found that treatment with Rg3 significantly reduced the expression levels of Col I and Col III, which are the main ECM components that are excessively deposited in the vocal cord scar tissue. By inhibiting the synthesis of these key collagen molecules, Rg3 effectively alleviated the excessive deposition of the extracellular matrix, which is crucial for restoring the normal structure and vibration characteristics of the vocal cord.

The results of this study indicate that ginsenoside Rg3 exerts dual regulatory effects on HVFSFs, providing important insights into its therapeutic mechanism. Firstly, Rg3 dose-dependently inhibited HVFSFs proliferation and significantly promoted cell apoptosis. The caspase (cysteine-dependent aspartate-directed protease) family serves as a core component of apoptotic signaling pathways, with caspase-3 regarded as the key executioner of apoptosis; its activation marks an irreversible commitment to cell death.[16] Western blot and qPCR analyses confirmed that caspase-3 expression was significantly upregulated following Rg3 treatment, suggesting that Rg3 may actively induce programmed cell death in over-proliferating vocal fold scar fibroblasts through activation of the caspase-3-dependent apoptotic pathway. Furthermore, the regulatory effect of Rg3 on collagen metabolism is particularly noteworthy. Rg3 treatment significantly reduced the expression levels of Col I and Col III, which are the main ECM components excessively deposited in vocal fold scar tissue. By inhibiting the synthesis of these key collagen molecules, Rg3 effectively alleviated excessive ECM deposition, which is crucial for restoring the normal structural architecture and vibratory characteristics of the vocal folds.

Although this discussion focuses on the caspase-3 pathway, intracellular signaling networks are complex and highly interconnected. Caspase-3 activation is frequently regulated by multiple upstream signaling pathways, including Bcl-2 family proteins[17] (modulating the mitochondrial apoptosis pathway) and the Fas/FasL system [18] (regulating the death receptor-mediated apoptosis pathway). Concurrently, Rg3 may exert anti-fibrotic effects synergistically with caspase-3 pathway activation by modulating other classical fibrosis-related pathways, such as TGF-β/Smad,[14] MAPK (mitogen-activated protein kinase),[12,19] and PI3K/Akt (phosphatidylinositol 3-kinase/protein kinase B).[20-22] For instance, Rg3 may inhibit TGF-β1 expression or receptor activation, thereby attenuating pro-fibrotic signaling[23] - an effect that may occur independently of or in synergy with its pro-apoptotic actions. Future studies should comprehensively elucidate the complete signaling network through which Rg3 exerts its effects in HVFSFs.

Conclusion

In conclusion, our findings highlight ginsenoside Rg3 as a promising candidate for anti-fibrotic therapy in vocal fold scarring, given its dual ability to induce fibroblast apoptosis and suppress pathological collagen deposition. Further in vivo studies and clinical trials are warranted to validate its therapeutic potential.

Acknowledgements

This work was supported by the Yichang Medical and Health Research Project(A23-1-024)

Author Contributions

Conceived and designed the experiments: Jun Liu, Long Zhang. Performed the experiments: Yan Qin, Kang Wang, Zhi-Mao Zhang. Analyzed the data: Ting Wu. Contributed reagents/materials/analysis tools: Kang Wang, Zhi-Mao Zhang, Wu Ting. Writing the paper: Yan Qin, Jun Liu, Long Zhang.

References

1. Yang Y, Xu X, Zhuang P. Explore the Pattern of Biomechanical Alterations in Vocal Fold Scar and Its Objective Quantitative Assessment Method. J Voice. 2024 Jul 24:S0892-1997(24)00212-1. doi: 10.1016/j.jvoice.2024.07.003. Epub ahead of print. PMID: 39054187.
2. Miura R, Matsuzaki H, Suzuki H, Makiyama K, Oshima T. Effect of a Single Injection of Basic Fibroblast Growth Factor into the Vocal Folds: A 36-Month Clinical Study. J Voice. 2023 May;37(3):444-451. doi: 10.1016/j.jvoice.2021.01.015. Epub 2021 Feb 9. PMID: 33573843.
3. Vontela S, Balouch B, Bress E, Brennan MJ, Alnouri G, Martha VV, Sataloff RT. Vocal Fold Paresis and Voice Outcomes following Vocal Fold Mass Excision. J Voice. 2024 Jan;38(1):225-230. doi: 10.1016/j.jvoice.2021.07.014. Epub

2021 Aug 30. PMID: 34474936.
4. Kang HT, Park KN, Lee SW. Regenerative Effect of a 532-nm Diode Laser on Vocal Fold Scar in a Rabbit Model. J Voice. 2026 Jan;40(1):160-166. doi: 10.1016/j.jvoice.2023.09.004. Epub 2023 Oct 29. PMID: 37903688.
5. Svistushkin MV, Kotova S, Shpichka A, Starostina S, Shekhter A, Bikmulina P, Nikiforova A, Zolotova A, Royuk V, Kochetkov PA, Timashev S, Fomin V, Vosough M, Svistushkin V, Timashev P. Stem cell therapy for vocal fold regeneration after scarring: a review of experimental approaches. Stem Cell Res Ther. 2022 May 3;13(1):176. doi: 10.1186/s13287-022-02853-9. PMID: 35505357; PMCID: PMC9066721.
6. John M, Nabizath A, Krishnakumar S, Menon U, Menon D, Nair M. Injectable Tissue Adhesive Microgel Composite Containing Antifibrotic Drug for Vocal Fold Scarring. ACS Appl Bio Mater. 2024 Aug 19;7(8):5237-5246. doi: 10.1021/acsabm.4c00422. Epub 2024 Jul 15. PMID: 39007499.
7. Pierce JL, Olson B, Merrill RM, Pierce J, Isom A, Torrecillas V, McCrary H, Aylward A, Smith ME, Ben Christensen M. Amniotic Fluid as a Potential Treatment for Vocal Fold Scar in a Rabbit Model. J Voice. 2025 Jan 3:S0892-1997(24)00445-4. doi: 10.1016/j.jvoice.2024.12.015. Epub ahead of print. PMID: 39755523.
8. Halder N, Perkerson R, Kanekiyo T, Rutt AL. Compatibility of Hepatocyte Growth Factor, Adipose-Derived Mesenchymal Stem Cells, and Dermal Fillers for the Treatment of Vocal Fold Scar. Stem Cell Rev Rep. 2025 May;21(4):1131-1133. doi: 10.1007/s12015-025-10862-3. Epub 2025 Feb 28. PMID: 40019729.
9. Wu L, Bai L, Dai W, Wu Y, Xi P, Zhang J, Zheng L. Ginsenoside Rg3: A Review of its Anticancer Mechanisms and Potential Therapeutic Applications. Curr Top Med Chem. 2024;24(10):869-884. doi: 10.2174/1115680266283661240226052054. PMID: 38441023.
10. Yao ZW, Zhu H. Pharmacological mechanisms and drug delivery systems of ginsenoside Rg3: A comprehensive review. Pharmacol Res. 2025 Jun;216:107799. doi: 10.1016/j.phrs.2025.107799. Epub 2025 May 23. PMID: 40414584.
11. Tian ZF, Hu RY, Wang Z, Wang YJ, Li W. Molecular mechanisms behind the inhibitory effects of ginsenoside Rg3 on hepatic fibrosis: a review. Arch Toxicol. 2025 Feb;99(2):541-561. doi: 10.1007/s00204-024-03941-w. Epub 2024 Dec 27. PMID: 39729114.
12. Chen Y, Peng Y, Li P, Jiang Y, Song D. Ginsenoside Rg3 induces mesangial cells proliferation and attenuates apoptosis by miR-216a-5p/MAPK pathway in diabetic kidney disease. Aging (Albany NY). 2024 Jun 7;16(11):9933-9943. doi: 10.18632/aging.205907. Epub 2024 Jun 7. PMID: 38850526; PMCID: PMC11210261.
13. Yun E, Kwon BS, Kim J, Lee A. Ginsenoside Rg3 attenuates pulmonary fibrosis by inhibiting endothelial to mesenchymal transition. Anim Cells Syst (Seoul). 2023 Aug 4;27(1):159-170. doi: 10.1080/19768354.2023.2244549. PMID: 37554358; PMCID: PMC10405771.
14. Tang M, Bian W, Cheng L, Zhang L, Jin R, Wang W, Zhang Y. Ginsenoside Rg3 inhibits keloid fibroblast proliferation, angiogenesis and collagen synthesis in vitro via the TGFβ/Smad and ERK signaling pathways. Int J Mol Med. 2018 Mar;41(3):1487-1499. doi: 10.3892/ijmm.2018.3362. Epub 2018 Jan 4. PMID: 29328420; PMCID: PMC5819908.
15. Naba A. Mechanisms of assembly and remodelling of the extracellular matrix. Nat Rev Mol Cell Biol. 2024 Nov;25(11):865-885. doi: 10.1038/s41580-024-00767-3. Epub 2024 Sep 2. PMID: 39223427; PMCID: PMC11931590.
16. Eskandari E, Eaves CJ. Paradoxical roles of caspase-3 in regulating cell survival, proliferation, and tumorigenesis. J Cell Biol. 2022 Jun 6;221(6):e202201159. doi: 10.1083/jcb.202201159. Epub 2022 May 12. PMID: 35551578; PMCID: PMC9106709.
17. Liang Z, Chen Y, Gu R, Guo Q, Nie X. Asiaticoside Prevents Oxidative Stress and Apoptosis in Endothelial Cells by Activating ROS-dependent p53/Bcl-2/Caspase-3 Signaling Pathway. Curr Mol Med. 2023;23(10):1116-1129. doi: 10.2174/1566524023666221024120825. PMID: 36284389.
18. Wang Z, Tan Y, Xu F. Zonisamide improves Fas/FasL-mediated apoptosis and inflammation in a degenerative cervical myelopathy rat model. Tissue Cell. 2023 Apr;81:102024. doi: 10.1016/j.tice.2023.102024. Epub 2023 Jan 13. PMID: 36669388.
19. Choi RJ, Mohamad Zobir SZ, Alexander-Dann B, Sharma N, Ma MKL, Lam BYH, Yeo GSH, Zhang W, Fan TP, Bender A. Combination of Ginsenosides Rb2 and Rg3 Promotes Angiogenic Phenotype of Human Endothelial Cells via PI3K/Akt and MAPK/ERK Pathways. Front Pharmacol. 2021 Feb 10;12:618773. doi: 10.3389/fphar.2021.618773. PMID: 33643049; PMCID: PMC7902932.
20. Wan J, Cheng W, Xing X, He Y, Tang P, Feng Y, Liu S, Lu X, Zhong L. A SERS-Based Dual-Parameter Monitoring Nanoprobe of ROS and PI3K/Akt during Ginsenoside Rg3-Induced Cell Apoptosis. Biosensors (Basel). 2023 Jan 31;13(2):212. doi: 10.3390/bios13020212. PMID: 36831977; PMCID: PMC9953484.
21. Tao D, Li F, Zhang X, Guo H, Yang R, Yang Y, Zhang L, Shen Z, Teng J, Chen P, He B. 20(R)-ginsenoside Rg3 protects against focal cerebral ischemia–reperfusion injury by suppressing autophagy via PI3K/Akt/mTOR signaling pathway. Neuropharmacology. 2025 Feb 1;263:110226. doi: 10.1016/j.neuropharm.2024.110226. Epub 2024 Nov 16. PMID: 39557153.
22. Wang X, He R, Geng L, Yuan J, Fan H. Ginsenoside Rg3 Alleviates Cisplatin Resistance of Gastric Cancer Cells Through Inhibiting SOX2 and the PI3K/Akt/mTOR Signaling Axis by Up-Regulating miR-429. Front Genet. 2022 Mar 3;13:823182. doi: 10.3389/fgene.2022.823182. PMID: 35309116; PMCID: PMC8927288.
23. Xu H, Miao H, Chen G, Zhang G, Hua Y, Wu Y, Xu T, Han X, Hu C, Pang M, Tan L, Liu B, Zhou Y. 20(S)-ginsenoside Rg3 exerts anti-fibrotic effect after myocardial infarction by alleviation of fibroblasts proliferation and collagen deposition through TGFBR1 signaling pathways. J Ginseng Res. 2023 Nov;47(6):743-754. doi: 10.1016/j.jgr.2023.06.007. Epub 2023 Jul 3. PMID: 38107395; PMCID: PMC10721484.

***Corresponding author:** Jun Liu. Department of Otorhinolaryngology Head and Neck Surgery, Yichang Central People's Hospital, The First College of Clinical Medical Science, China Three Gorges University. No.183 Yiling Avenue, Yichang City, Hubei Province, China. 443003. E-mail: dsgxliujun@163.com.*